Leukemia (2021) 35:679–690
https://doi.org/10.1038/s41375-020-0937-3

ARTICLE

Acute lymphoblastic leukemia

PRL3 enhances T-cell acute lymphoblastic leukemia growth through suppressing T-cell signaling pathways and apoptosis

E. G. Garcia[1,2,3,4] · A. Veloso[1,2,3,4] · M. L. Oliveira[5] · J. R. Allen[1,2,3,4] · S. Loontiens[6] · D. Brunson[1,2,3,4] · D. Do[1,2,3,4] · C. Yan[1,2,3,4] · R. Morris[2] · S. Iyer[1,2,3,4] · S. P. Garcia[1,2,3,4] · N. Iftimia[1,2,3,4] · W. Van Loocke[6,7] · F. Matthijssens[6,7] · K. McCarthy[1,2,3,4] · J. T. Barata[5] · F. Speleman[6,7] · T. Taghon[8] · A. Gutierrez[9] · P. Van Vlierberghe[6,7] · W. Haas[1,2,3,4] · J. S. Blackburn[10] · D. M. Langenau[1,2,3,4]

Received: 4 September 2019 / Revised: 10 June 2020 / Accepted: 16 June 2020 / Published online: 30 June 2020

Abstract

T-cell acute lymphoblastic leukemia (T-ALL) is an aggressive malignancy of thymocytes and is largely driven by the NOTCH/MYC pathway. Yet, additional oncogenic drivers are required for transformation. Here, we identify protein tyrosine phosphatase type 4 A3 (PRL3) as a collaborating oncogenic driver in T-ALL. PRL3 is expressed in a large fraction of primary human T-ALLs and is commonly co-amplified with MYC. PRL3 also synergized with MYC to initiate early-onset ALL in transgenic zebrafish and was required for human T-ALL growth and maintenance. Mass-spectrometry phosphoproteomic analysis and mechanistic studies uncovered that PRL3 suppresses downstream T-cell phosphorylation signaling pathways, including those modulated by VAV1, and subsequently suppresses apoptosis in leukemia cells. Taken together, our studies have identified new roles for PRL3 as a collaborating oncogenic driver in human T-ALL and suggest that therapeutic targeting of the PRL3 phosphatase will likely be a useful treatment strategy for T-ALL.

Supplementary information The online version of this article (https://doi.org/10.1038/s41375-020-0937-3) contains supplementary material, which is available to authorized users.

✉ D. M. Langenau
dlangenau@mgh.harvard.edu

1 Department of Pathology, Massachusetts General Research Institute, Boston, MA 02114, USA

2 Center of Cancer Research, Massachusetts General Hospital, Charlestown, MA 02129, USA

3 Harvard Stem Cell Institute, Boston, MA 02114, USA

4 Center of Regenerative Medicine, Massachusetts General Hospital, Boston, MA 02114, USA

5 Instituto de Medicina Molecular João Lobo Antunes Faculdade de Medicina, Universidade de Lisboa, Lisbon, Portugal

6 Cancer Research Institute Ghent, Ghent, Belgium

7 Department of Biomolecular Medicine and Center for Medical Genetics, Ghent University, Ghent, Belgium

8 Department of Diagnostic Sciences, Ghent University, Ghent, Belgium

9 Division of Hematology/Oncology, Boston Children's Hospital and Dana-Farber Cancer Institute, Boston, USA

10 Department of Molecular and Cellular Biochemistry, University of Kentucky College of Medicine, Lexington, KY 40536, USA

Introduction

T-cell acute lymphoblastic leukemia (T-ALL) affects thousands of children and adults each year in the United States [1, 2]. T-ALL initiates from T cells that accumulate genomic alterations and/or epigenetic changes that promote their transformation. Common genetic translocation events, point mutational activation of promoter elements, and super enhancer regulation elicit sustained expression of oncogenic transcription factors, including basic helix-loop-helix family members (TAL1), LIM-only family members (LMO1 and LMO2), homeobox family members (TLX1, TLX3, HOXA), and proto-oncogenes (c-MYB) [3, 4]. Aberrant T-ALL oncogene expression is also associated with developmental arrest and transformation of T cells at specific maturation states. Despite these molecular differences in T-ALL subtypes, it is also now widely recognized that the MYC transcription factor is a dominant oncogenic driver in a majority of human T-ALL and is often activated downstream of NOTCH1 [5–7]. MYC is also amplified as a large, single copy chromosomal gain in ~12% of human T-ALL. Despite the dominant role that the NOTCH/MYC oncogenic pathway plays in T-ALL, it is clear that additional oncogenic drivers collaborate to induce the transformation of thymocytes.

Standard treatment for T-ALL is high dose multi-agent chemotherapy combining drugs with distinct mechanisms of action, including anthracyclines, steroids, vincristine, asparaginase, cyclophosphamide, cytarabine, and methotrexate. However, these treatment regimens fail in ~20% of children and 50% of adults [1, 8, 9]. These refractory and relapse T-ALLs have a particularly poor prognosis [10, 11]. Thus, further understanding of the underlying molecular mechanisms driving T-ALL growth and maintenance is imperative for developing new, targeted therapeutic approaches. For example, Trinquand et al. have shown that re-activation of T-cell receptor (TCR)-signaling can kill T-ALL cells, suggesting hyperactivation of TCR or its downstream phosphorylation substrates could be novel therapeutic targets in human T-ALL [12].

Phosphatases have important roles in regulating a wide array of developmental and cancer processes. Although classically thought of as tumor suppressors [13], an emerging subset of phosphatases has been identified as oncogenes. Protein tyrosine phosphatase type 4 A3 (also known as *PRL3*) is one such phosphatase. It encodes a small 21 kDa phosphatase that has been implicated in regulating tumor maintenance and metastasis in colorectal cancer [14], gastric carcinoma [15], hepatocellular carcinoma [16], and breast cancer [17]. PRL3 is a tyrosine phosphatase that alters several major signaling pathways including Rho GTPases and Src [18, 19]. Interestingly, PRL3 contains a single catalytic domain and a c-terminal CAAX prenylation motif that is important for intracellular localization and membrane association [20, 21]. To date, roles for PRL3 in regulating T-ALL growth and maintenance have not been determined. Moreover, synergies between MYC and PRL3 in cancer have not been described nor have the downstream pathways regulated by PRL3 been fully elucidated.

Here, we identify PRL3 as a critical driver of leukemia growth in both zebrafish and human T-ALL. PRL3 is highly expressed in a large fraction of human T-ALL and synergizes with MYC to initiate early-onset and aggressive leukemia in transgenic zebrafish. Chemical and genetic loss-of-function studies uncovered that PRL3 is also required for continued human T-ALL growth and maintenance. Following unbiased mass-spectrometry phosphoproteomic analysis, we next uncovered that PRL3 suppresses T-cell signaling pathways by dampening the activity of key proteins required for signal transduction, including VAV1. Functional studies confirmed that PRL3 regulates well-known phosphorylation targets of TCR activation and suppresses apoptosis. In total, our studies have identified new roles for PRL3 in regulating the onset and growth of T-ALL and uncovered unanticipated downstream molecular mechanisms underlying its role in T-ALL maintenance.

Materials and methods

Patient samples and genomic analyses

Diagnostic T-ALL lymphoblast specimens were collected from children enrolled on Dana-Farber Cancer Institute study 05-001 (https://clinicaltrials.gov/ct2/show/NCT00400946) or Children's Oncology Group clinical trial AALL0434 (https://clinicaltrials.gov/ct2/show/NCT00408005). Lymphoblasts were purified using Ficoll-Paque reagent, genomic DNA was extracted, and copy number analysis was performed by array CGH analysis, essentially as described [22]. Gains were defined by a log2 copy number of >0.3. Array CGH data are available in the NCBI Gene Expression Omnibus (https://www.ncbi.nlm.nih.gov/geo/) as GSE96624.

Targeted exon sequencing was performed on a panel of genes with known roles in oncogenesis using the Dana-Farber OncoPanel massively parallel sequencing assay [23]. Mutations calls were made for single nucleotide variants using MuTect v1.1.4, for insertions/deletions using the SomaticIndelDetector tool of GATK, and mutation calls were made as described [23].

Zebrafish

DNA constructs have been described previously [24] with exception of *rag2-prl3,* which was created by PCR amplification of the zebrafish *prl3* and gateway cloning into the *rag2* destination vector. Plasmids were linearized with *NotI* or *XhoI*, purified, and injected into CG1-strain zebrafish [24]. In total, 20 ng/μl *rag2-Myc* was complexed with (1) 40 ng/μl of *rag2-GFP* or (2) 20 ng/μl r*ag2-prl3* plus 20 ng/μl of *rag2-mCherry*. Mosaic transgenic zebrafish were scored for fluorescent-labeled thymocytes at 21 days of life and every 7 days subsequently for disease onset. Leukemic fish were defined as >50% of their body infiltrated with fluorescent T-ALL cells [24]. Cell transplantation was completed essentially as described [25]. Zebrafish experiments were approved under animal protocol #2011-N-000127 (Massachusetts General Hospital).

Histology

A portion of each leukemic fish was fixed in 4% paraformaldehyde, embedded in paraffin, sectioned, and stained with hematoxylin and eosin, anti-cleaved caspase-3 and anti phosphohistone H3 [24, 25]. The ratio of positively stained cells to unstained cells was calculated in three separate areas

of each tumor. Significance was calculated by Student's *t* test.

T-ALL cell lines and lentiviral infections

Human T-ALL cell lines were obtained from ATCC or DSMZ. All cell lines were authenticated just prior to use in experiments using FTA sample collection kit for human cell authentication service from ATCC and certified Mycoplasma-free (MycoAlert Plus, Lonza, Basel, Switzerland; tested every 6 months).

Knockdown experiments were performed using lentiviral vectors: pLKO-shScramble (CCTAAGGTTAAGTCGCCC TCGCTCGAGCGAGGGCGACTTAACCTTAGG), pLKO-shPRL3#1 (GTGTGTGAAGTGACCTATGACCTCGAGG TCATAGGTCACTTCACACAC) or pLKO-shPRL3#2 (AG CTCACCTACCTGGAGAAATCTCGAGATTTCTCCAGG TAGGTGAGCT). Transduced T-ALL cells were washed 24 h post infection and cultured normally. Knockdowns were confirmed by western blot analysis as outlined below.

Mice xenograft studies and bioluminescence imaging

Human Jurkat T-ALL cells were luciferized using the pLKO.1-luciferase-mKate. A total of 1×10^6 luciferized control shSCR, shPRL3#1, or shPRL3#2 cells were injected with an equal volume of matrigel (Thermo Fisher Scientific, Pittsburgh, Pennsylvania) into the flanks of 6-week-old NOD/SCID/IL2Rγ-null female mice (100 µl/mice). Following engraftment, mice were anesthetized by isoflurane and monitored by bioluminescence imaging. Statistical analysis was completed using the Student's *t* test. Mouse experiments were approved under animal protocol #2009-P-002756 (Massachusetts General Hospital).

Inhibitor drugs

PRL3 activity was inhibited using rhodanine derivative PRL3 inhibitor (P0108, Sigma-Aldrich, St. Louis, Missouri). Cell apoptosis was inhibited using caspase-3 (Z-DEVD-FMK, S7312, Selleck Chemicals, Houston, TX) and pan-caspase (Z-VAD-FMK, Selleck S7023) small molecules at 50 µM.

Flow cytometry and analysis

T-cell activation was assessed by flow cytometry using the following fluorescent-conjugated antibodies: CD69-Brilliant Violet 421 (BioLegend 310929, Dedham, MA), CD25-PerCP Cy5.5 (aka IL2RA BioLegend 302626), and HLA-DR-APC (BioLegend 307610). Cell cycle was assessed using the Click-It EdU Kit (Life Technologies, Carlsbad, California). A pulse of EdU was performed 1 h at 37 °C 4%CO_2 prior to cell harvest and preserved for immunofluorescent staining with Cytofix fixation buffer for 15 min at 37 °C (BD Biosciences, San Jose, California). Apoptosis was assessed using 7AAD (2.5 µl) plus Alexa Fluor 647-conjugated Annexin-V (2.5 µl) in the presence of 1X Annexin-V staining buffer (Life Technologies). All flow cytometry experiments were completed using either the LSR II or Fortessa Flow Cytometer (BD biosciences).

Western blot analysis and antibody reagents

Western blot analysis used the following rabbit anti-human antibodies: PRL3 (GTX 100600, VWR # 89307-822, Radnor, Pennsylvania), VAV1 (Cell Signaling Technology #2502, Danvers, Massachusetts), Pan pY (Cell Signaling Technology #8954), and GAPDH (Cell Signaling Technology #2118), CBL (Cell Signaling Technology # 2747), CBL pY674 (Abcam # ab76536, Cambridge, UK), ITK (Cell Signaling Technology # 77215S), ITK pTyr512 (Life Technologies #PA564523), LAT pY255 (Thermo Fisher Scientific # PIPA564800), LAT (Cell Signaling Technology # 9166S). Antibody binding was visualized with anti-rabbit HRP and developed by either Amersham ECL Prime reagent (GE Healthcare, Buckinghamshire, UK) or Super-Signal West Femto Chemiluminescent Substrate (Thermo Fisher Scientific) using a Fluor-S Multi-Imager (Bio-Rad, Hercules, California).

LC/MS-MS

Molt4 cells were serum starved for 24 h prior to PRL3 inhibitor exposure. PRL3 inhibitor was added to cells and harvested at 0, 5, 15, 30, and 60 min and 3, 6, and 24 h. DMSO-treated control cells were harvested at 0 and 24 h post treatment. Cells were washed twice with 1× TBS, pelleted, and flash frozen at −80 °C. LC/MS-MS was performed and is fully described in Supplementary methods. Four significant k-Means clusters were identified based on containing >10% of phosphopeptides having a >1.5 fold change at one time point when compared with control treated cells. This combined gene list was used in both the STRING and DAVID analysis.

VAV1 gain-of-function experiments

pMXspuro-GFP empty control was a gift from Jayanta Debnath (74203; http://n2t.net/addgene:74203; RRID: Addgene_74203136, Watertown, MA). pMX Vav1 uGFP (Addgene 14557) and pMX VAV1 Y3F uGFP (Addgene 14558) were a gift from Joan Brugge (Addgene 14557; http://n2t.net/addgene:14557 or 14558 [26]; RRID:Addgene_14557

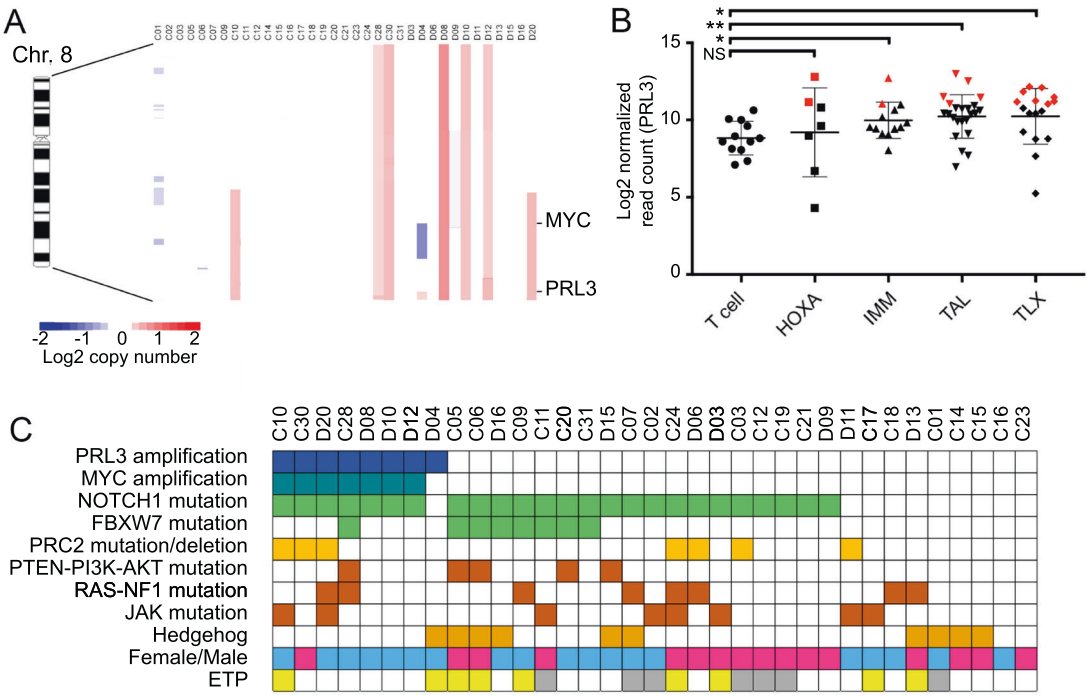

Fig. 1 PRL3 is co-amplified with MYC and highly expressed in subset of human T-ALL. a DNA copy number assessed by array comparative genomic hybridization (aCGH) in diagnostic T-ALL clinical specimens. The aCGH data are shown as a dChip plot of segmented log2 copy number ratios, with color representing the log2 copy number ratio (legend shown in bottom left). **b** PRL3 expression in 72 primary patient samples following RNA sequencing. Samples that expressed PRL3 at two standard deviations higher than normal thymocytes are denoted by red coloring. * denotes $p < 0.05$ and ** denotes $p < 0.01$ by Student's t test. NS Not significant. **c** Summary of genetic alterations identified in primary T-ALL samples following array CGH and targeted exome sequencing.

or 14558). pMX VAV1 uGFP was modified to express VAV1 Y826F using constructs manufactured by Integrated DNA Technologies (IDT, Coralville, Iowa).

VAV1 constructs were nucleofected into Jurkat and KE37 human T-ALL cells using the Amaxa Cell Line Nucleofector Kit V (program X-001 was used for Jurkat; program A-030 was used for KE37; Lonza, Basel, Switzerland). Transfected cells were analyzed for T-cell activation and apoptosis by flow cytometry as outlined above. Statistical analysis was completed using the Student's t test.

Results

PRL3 is amplified with MYC and expressed in a subset of human T-ALLs

Analysis of human T-ALL samples by array comparative genomic hybridization (aCGH) revealed that *MYC* was also commonly co-amplified with *PRL3* (8q24.3; Fig. 1a, $n = 7$ of 35). In addition, RNA sequencing of primary patient samples revealed that 24% of human T-ALL patients express two standard deviations (SD) higher *PRL3* transcripts when compared with normal T cells (Fig. 1b, $n = 17$ of 72, $p < 0.05$, Student's t test). Most human T-ALLs have oncogenic activation of the NOTCH/MYC pathway, suggesting that PRL3 and MYC might collaborate to induce leukemia even in the absence of chromosome amplification. Consistent with this observation, *PRL3* expression was not confined to a specific molecular subtype of disease (Fig. 1b). Finally, aCGH analysis when combined with targeted exome sequencing of primary patient leukemias revealed that PRL3 and MYC copy number gains co-occurred with a number of classical T-ALL mutations such as those involving NOTCH1, genes of the Polycomb repressive complex 2 (PRC2), or JAK pathway genes. Yet, there was no significant association of PRL3 amplification with specific gene mutations (Fig. 1c). Together, we conclude that *PRL3* is amplified with *MYC* in a subset of human T-ALLs and yet transcriptionally regulated in a larger fraction of human T-ALLs.

prl3 collaborates with Myc to accelerate ALL onset in transgenic zebrafish

Given the association of MYC amplification with PRL3 in human T-ALL, we next wanted to assess the collaborative oncogenic potential for these factors in vivo. CG1-strain syngeneic zebrafish were injected at the one-cell stage with *rag2-Myc*, *rag2-prl3*, or both transgenes together. Because

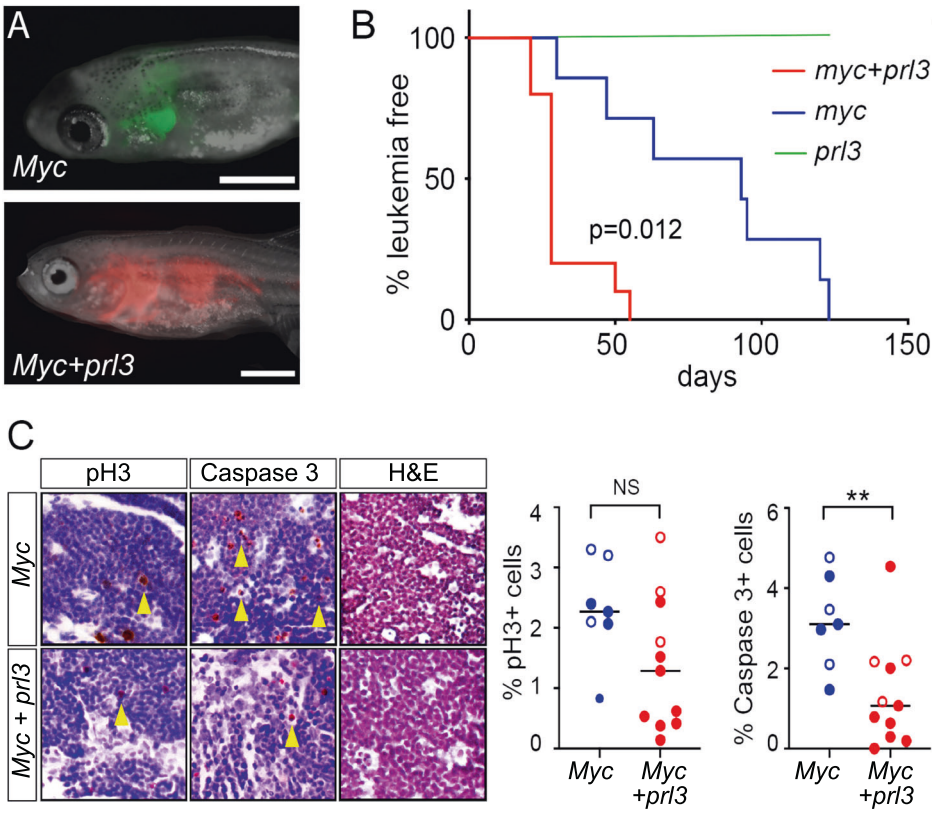

Fig. 2 Prl3 collaborates with Myc to accelerate T-ALL onset and suppresses apoptosis in transgenic zebrafish. a Syngeneic CG1 fish injected at the one-cell stage with *rag2-Myc* or *rag2-prl3* and *rag2-Myc* in combination. Representative images of mosaic transgenic zebrafish shown at 28 days post injection. **b** Kaplan–Meier analysis of leukemic fish ($p = 0.012$ comparing *Myc, prl3* and *Myc*+prl3-expressing T-ALL, log-rank statistic). $n \geq 7$ animals/arm. **c** Histological analysis of representative T-ALL. Hematoxylin and eosin stained sections juxtaposed to immunohistochemistry for phospho-H3 and cleaved caspase-3. Yellow arrowheads denote examples of positively stained cells. (Right) Quantification of IHC data where each datum point represents a single primary T-ALL (filled) or transplanted leukemia (open). **Denote $p < 0.01$ by Student's *t* test. NS not significant. Scale bar equals 0.1 cm.

animals were also co-injected with a fluorescent reporter transgene, mosaic transgenic zebrafish could be followed for leukemic cell transformation using whole animal epi-fluorescent stereomicroscopy beginning at 21 days of life (Fig. 2a). These analyses showed that *prl3* was not oncogenic on its own and instead collaborated with *Myc* to accelerate time of leukemia onset ($p = 0.008$, log-rank statistic, Fig. S1A). Moreover, *prl3*-expressing leukemias were more aggressive and established disease in transplant recipients earlier than Myc alone expressing ALL (Fig. S1B; $p \leq 0.03$, log-rank statistic).

Because the *rag2-Myc* transgenic model develops T-ALL, B-ALL, and MPAL [25, 27, 28], we next performed RNAseq analysis on primary and transplanted ALLs to assign leukemia subtype. Leukemias were assessed for well-known markers of T- and B-cell development and TCRb receptor re-arrangement (Fig. S1C, and Supplementary Table 1). These analyses identified that Myc-induced leukemias were largely T cell in origin ($n = 7$ were T-ALL, 1 was B-ALL, and 1 was mixed lineage leukemia). prl3-expressing leukemias were also comprised of T ($n = 9$), B ($n = 4$), and mixed cell lineage leukemias ($n = 3$). There was no statistical difference in overall leukemia spectrum or clonality of Myc vs. Myc+prl3-expressing ALLs ($p = 0.264$, and $p = 0.637$, respectively, Fisher exact test). Kaplan–Meier analysis was next performed based on lineage calls and confirmed that prl3 collaborated with Myc to specifically induce early-onset and aggressive T-ALL ($p = 0.012$, log-rank statistic, Fig. 2b). To determine the underlying differences in prl3-expressing T-ALL, we next assessed leukemias for differences in proliferative capacity and apoptosis. Immunohistochemistry (IHC) for phosphohistone-H3 showed no appreciable difference in proliferation between Myc and Myc+prl3-expressing T-ALL (Fig. 2c). However, IHC for cleaved caspase-3 showed a dramatic threefold decrease in apoptotic cells in the *Myc*+prl3-expressing T-ALLs (Fig. 2c; $p < 0.01$, Student's *t* test). Together, these results establish that Myc and prl3 collaborate in vivo to induce early-onset T-ALL by specifically suppressing apoptosis.

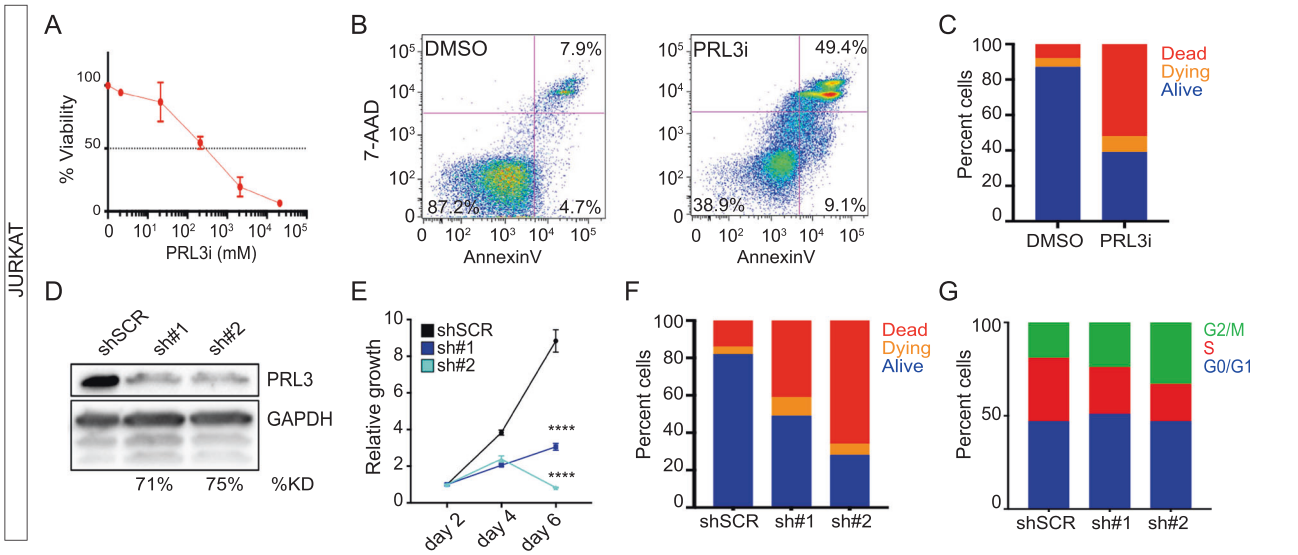

Fig. 3 PRL3 is required for human T-ALL viability and suppresses apoptosis. Cell viability and apoptosis following treatment of Jurkat T-ALL cells with the PRL3-inhbitior 1-(2-Bromobenzyloxy)-4-bromo-2-benzylidene rhodanine for 6 days (**a-c**) or following shRNA knockdown of PRL3 (**d–g**; 4 days (**d**) or 6 days after knockdown (**f**, **g**)). Cell titer glo (**a**, **e**), Flow cytometry analysis (**b**), and quantitation of Annexin-V/7AAD staining (**c**, **f**). Dead (Annexin-V$^+$/7AAD$^+$ cells), dying (Annexin-V$^+$/7AAD$^-$ cells), and alive (Annexin-V$^-$/7AAD$^-$ cells) cells are denoted. Western blot analysis following shRNA knockdown with percent knockdown noted at 4 days (**d**). Quantitation of EdU cell cycle analysis (**g**). ****Denotes $p < 0.0001$ by Student's t test comparison to control shRNA treated cells. Representative examples of three replicates are shown in all panels.

PRL3 is required for human T-ALL growth and inhibits cellular apoptosis

To assess if PRL3 also has roles in continued human T-ALL growth and maintenance, we next assessed the consequences of PRL3 inhibition in human T-ALL cells. PRL3-expressing Jurkat, Molt4, and KE37 T-ALL cells were treated with varying doses of the PRL3-inhibitior 1-(2-Bromobenzyloxy)-4-bromo-2-benzylidene rhodanine and compared with DMSO control. After six days of PRL3 inhibitor (PRL3i) treatment, all three T-ALL cell lines had reduced viability when assessed by cell titer glo (Fig. 3a and Fig. S2) and subsequently increased apoptosis when assessed by Annexin-V/7AAD staining (Fig. 3b, c and Fig. S2). To verify PRL3i effects on T-ALL growth, experiments were repeated using two PRL3-specific short hairpin RNAs (shRNA) and compared with control scramble (SCR) shRNA (Fig. 3d–g and Fig. S2). Both western blot analysis and quantitative real-time PCR confirmed efficient and specific knockdown of PRL3 but not related family members (Fig. 3d, Figs. S2, and S3). Following genetic knockdown of PRL3, all three T-ALL cell lines had reduced viability and increased apoptosis, but exhibited no consistent effect on cell cycle.

To extend our findings to the in vivo setting, PRL3 was knocked down in Jurkat cells and simultaneously transduced with luciferase to enable bioluminescence detection of leukemia growth when introduced into NOD/SCID/IL2rγ-null mice (Fig. 4 and Fig. S4). As was seen in cell culture experiments, PRL3 knockdown significantly reduced the growth of T-ALL by 14 days post transplant with differences in growth rates being observed until animals were sacrificed at 35 days post transplantation (Fig. 4b; $p < 0.05$, Student's t test). These results confirm roles for PRL3 in continued growth of human T-ALL.

PRL3 suppresses TCR signaling and subsequent downstream activation of apoptosis

To elucidate the downstream molecular mechanisms of PRL3, T-ALL cells were treated with PRL3i and then assessed for global differences in tyrosine phosphorylation over time. Specifically, Molt4 cells were serum starved for 24 h and then treated with 2 μM PRL3i. Cells were harvested at 0, 5, 15, 30, and 60 min and 3, 6, and 24 h after treatment. Samples were then subjected to total protein extraction and phosphorylated residues enriched by immunoprecipitation with total phospho-tyrosine antibody. Quantitative, isobaric labeling, and tandem mass spectrometry was then performed and identified 130 tyrosine-phosphorylated peptides that were significantly changed in comparing PRL3i-treated and control treated cells. These peptides came from 108 individual proteins and were activated in four distinct, temporal phosphorylation waves (Fig. 5, Supplementary Table 2). STRING analysis identified signaling nodes regulated by PRL3 that included TCR

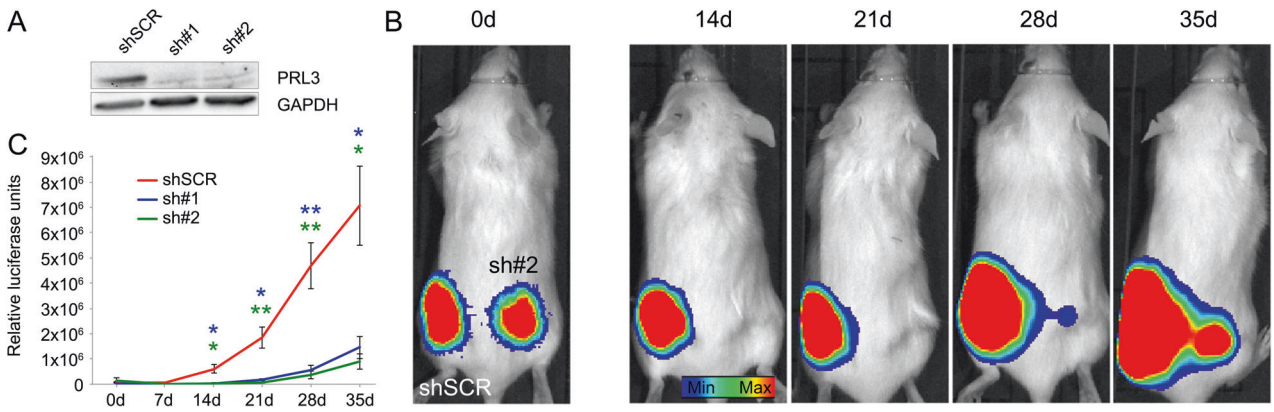

Fig. 4 PRL3 is required for human T-ALL growth and maintenance in mouse xenograft studies. a Western blot analysis following shRNA knockdown in Jurkat cells. **b** Luciferase bioluminescent imaging of representative animal engrafted with scramble control shRNA (shSCR, left flank) compared with shRNA to PRL3 (sh#2, right flank). High exposure images shown on 0 day to ensure equal injection of control and knockdown cells (left panels). Animals shown at different exposure from 14–35 days to highlight relative differences in growth between control and knockdown cells (right panels). **c** Quantification of growth at different time points. $*p < 0.05$, $**p < 0.01$, Student's t test. Error bars denote standard error of the mean. $N \geq 5$ mice/experimental arm.

signaling and splicing components (Fig. 5). To account for possible experimental bias in comparing phosphoproteins to the whole proteome using STRING, we also analyzed our data using DAVID. Along with analysis of additional phospho-serine and phospho-threonine peptide sites (Supplementary Table 3), these analyses independently identified that PRL3-inhibitor treatment had potent and significant effects on both classically defined downstream phosphorylation substrates of TCR signaling and RNA splicing (Supplementary Table 4). Importantly, well-known tyrosine-phosphorylated proteins implicated in TCR activation were identified in all four tyrosine-phosphorylation waves including VAV1 (Y826), LAT (Y255), CBL (Y669 and Y674), PLCγ1 (Y775 and Y783), and CD3D (Y160, Fig. 5b). Western blot analysis verified inhibitor effects on a subset of these downstream targets in the Molt4 cell line, independently confirming that PRL3 inhibitor effects had durable consequences for sustained TCR-associated signaling (Fig. S5B). Despite the clear role PRL3 had in regulating downstream TCR substrates, Molt4 cells fail to express membrane-localized TCR and thus cannot signal through classic TCR mediated signaling [29]. These results were entirely unexpected and showed that PRL3 regulates classically defined downstream phosphorylation cascades independent of an intact TCR.

To independently verify that PRL3 regulates downstream phosphorylation of classically defined downstream TCR signaling pathways, we next assessed human T-ALL cells for responses to PRL3 inhibitor treatment followed by flow cytometry for cell surface expression of cluster of differentiation 69 (CD69), interleukin 2 receptor alpha (IL2RA), and human leukocyte antigen DR isotype (HLA-DR). CD69 is one of the earliest cell surface antigens expressed by TCR-activated T cells, while IL2RA and HLA-DR are expressed at later stages of TCR activation [30]. Flow cytometry analysis confirmed that Jurkat, Molt4, and KE37 exhibited robust downstream activation of classically regulated TCR molecules following 4 days of PRL3 inhibitor treatment (Fig. 6a and Fig. S6) and led to increased apoptosis by 6 days of treatment when assessed by Annexin-V/7AAD staining (Fig. 6b and Fig. S6; $p < 0.0001$ Student's t test). These analyses were particularly exciting because only Jurkat cells express a functional TCR [29], while both Molt4 and KE37 lack functional TCR. These results again show that PRL3 inhibits the nucleation of downstream TCR phosphorylation substrates independently of a fully formed, membrane localized TCR. To independently confirm these results, genetic loss-of-function studies were performed in T-ALL cells using shRNA knockdown. Again, genetic knockdown of PRL3 resulted in elevated downstream TCR signaling after 4 days of shRNA treatment and subsequent induction of apoptosis in all three T-ALL cell lines by 6 days (Fig. 6c, d and Fig. S6). shRNA knockdown of PRL3 also resulted in robust phosphorylation of well-known TCR phosphorylation target proteins, including LCK (pTy394), ZAP-70 (pTy492), and PLCg1 (pTy783, Fig. S5C). Finally, we evaluated the effect of caspase-3 and pan-caspase inhibitor treatment in PRL3 knockdown T-ALL cells. Flow cytometry analysis revealed that PRL3-knockdown cells failed to undergo apoptosis when grown in the presence of caspase inhibitors (Fig. S7). Yet, these cells exhibited robust and elevated downstream T-cell activation as assessed by cell surface expression of IL2RA and HLA-DR. Together, these experiments confirm that PRL3 inactivation results in downstream TCR tyrosine-phosphorylation signaling and subsequently the induction of apoptosis.

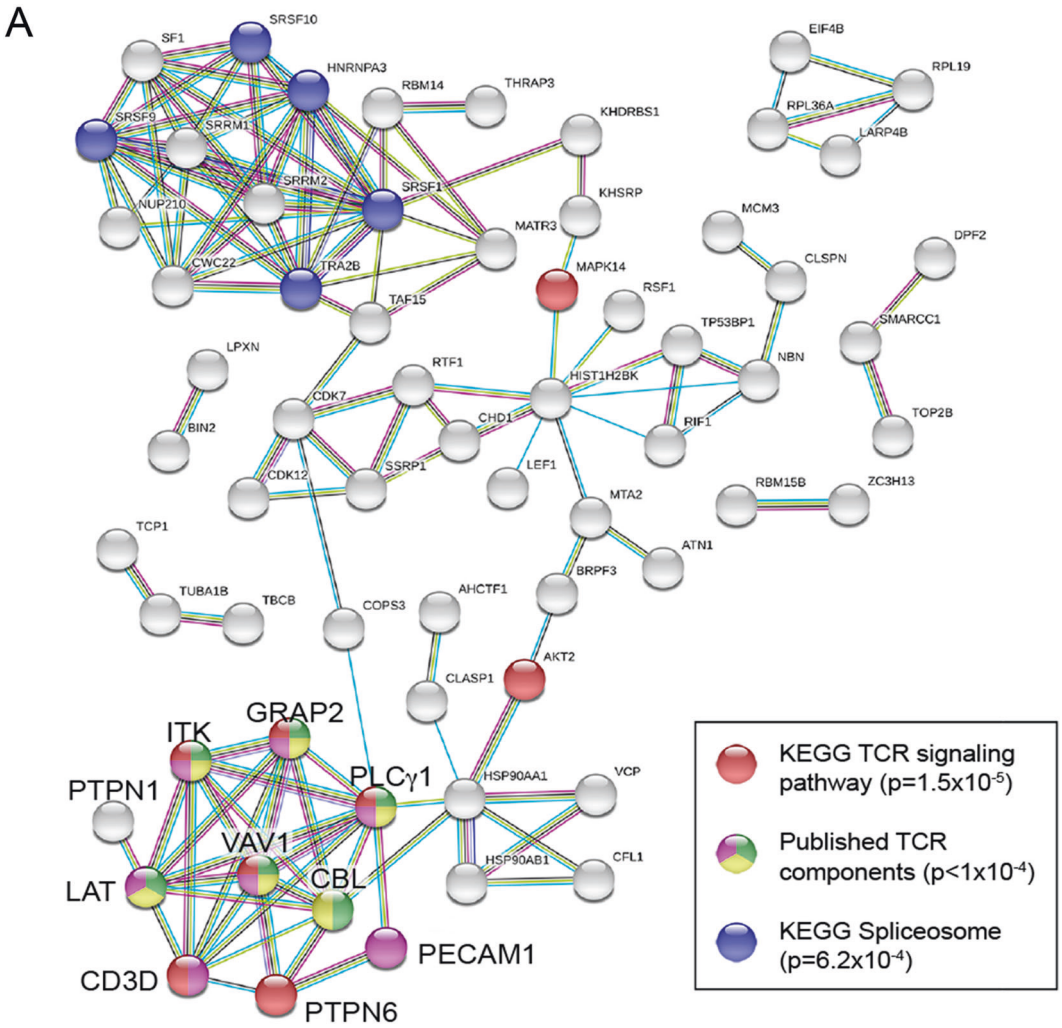

B

Protein	pY	Function
VAV1	pY826	GEF protein required for downstream TCR signaling
LAT	p255	ZAP70 kinase substrate in TCR signaling
GRAP2	pY45	Adaptor protein invovled in TCR signaling
CBL	pY669, pY674	Ubiquitin ligase regulated by TCR signaling
PLCγ1	pY775, pY783	Phospholipase induced by and regulates TCR signaling
ITK	pY512	Kinase that functions downstream of TCR to regulate PLCγ1
PTPN6	pY536; pY564	Phosphatase regulated downstream of TCR signaling
CD3D	pY160	Binds directly to TCR to regulate signaling

Fig. 5 Quantitative mass-spectrophotometry analysis identifies that PRL3 suppresses classically defined T-cell receptor phosphorylation signaling pathways. a STRING network analysis using all 130 identified phosphoproteins. Significantly enriched kyoto encyclopedia of genes and genomes (KEGG) pathways are color coded. T-cell receptor signaling pathway (hsa04660), Splicesome (hsa03040) and known associations identified in reference publications annotated within the STRING program. Pathway enrichment is denoted by *p* values provided within the key. **b** TCR downstream signaling proteins and specific peptide residues that were significantly phosphorylated following PRL3i treatment. Colored bar to left indicates the phosphorylation cluster of each peptide. Early induced phosphorylation events are noted by blue, while latter waves of phosphorylation are noted by green shades and red.

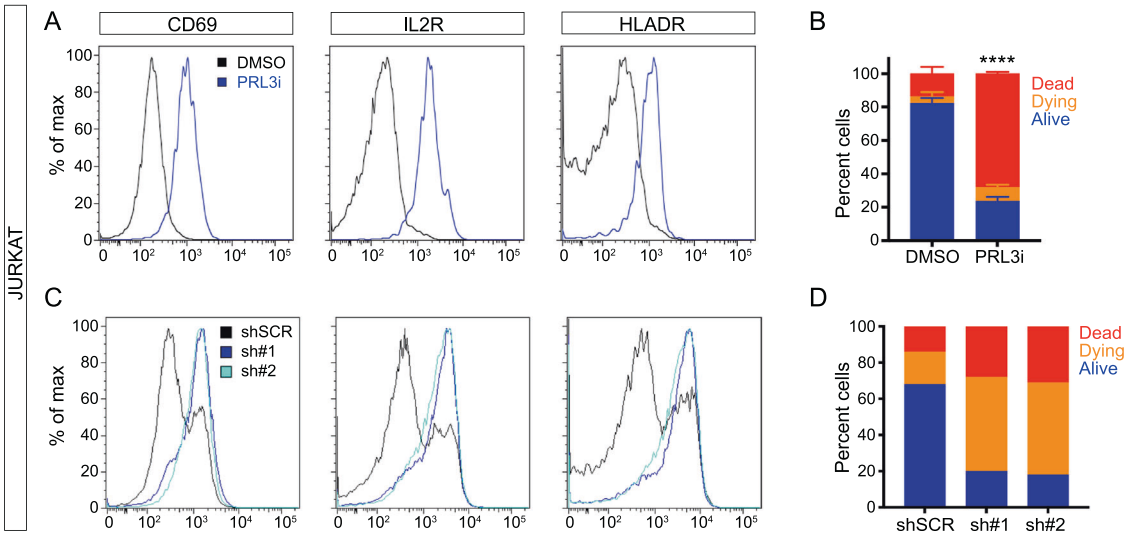

Fig. 6 PRL3 inhibition leads to downstream T-cell receptor pathway activation and subsequent induction of apoptosis in human T-ALL cells. a Flow cytometry analysis showing T-cell activation marker CD69, IL2RA, and HLA-DR expression following DMSO or PRL3i treatment for 4 days in Jurkat T-ALL cells. **b** Quantification of Annexin-V/7AAD staining following DMSO or PRL3i treatment for 6 days. Dead (Annexin-V + /7AAD +), dying (Annexin-V+/7AAD−), and alive (Annexin-V−/7AAD−). **** denote $p < 0.0001$ from three independent replicates. **c** Flow cytometry analysis showing T-cell activation marker CD69, IL2RA, and HLA-DR expression following scramble control (shSCR) or knockdown of PRL3 (sh#1 and sh#2) after 4 days of treatment. **d** Quantification of Annexin-V/7AAD staining following scramble control (shSCR) or knockdown of PRL3 (sh#1 and sh#2) after 6 days of treatment. Representative examples of three replicates are shown.

VAV1 is a guanine nucleotide exchange factor (GEF) for Rho-family GTPases that is required for TCR signaling [31–33]. Our mass-spec phoshoproteomics data identified the VAV1 Y826 residue as being rapidly phosphorylated after only 5 min of small molecule PRL3 inhibitor exposure (Fig. 5b and Supplementary Table 2). This residue is critical to controlling GEF activity [34], is required for efficient TCR signaling, and is known to regulate activation of critical signaling molecules, including CD28, LAT, SYK, CSK, RAC, SLP-76, and ZAP-70 [34–38]. To assess direct downstream activation of classically defined TCR signaling by VAV1, we engineered T-ALL cells to express (1) empty vector control, (2) wild-type VAV1, (3) constitutively GEF-active VAV1 [26, 39], or (4) VAV1 that contains a Y826F mutation that inhibits GEF activity [34]. Importantly, these constructs co-expressed GFP, allowing us to analyze signaling only within GFP+ nucleofected cells. T-ALL cells were harvested at 1, 2, and 3 days following nucleofection and assessed for IL2RA and HLA-DR expression and apoptosis using Annexin-V/7AAD staining. As expected, constitutively active VAV1 resulted in elevated classically defined TCR signaling and subsequent induction of apoptosis (Fig. 7). By contrast, cells engineered to express only wild-type VAV1 or non-phosphorylatable, GEF-inactive VAV1 Y826F were largely unable to induce downstream TCR signaling and exhibited only minimal effects on inducing apoptosis (Fig. 7). Together, these genetic gain-of-function experiments confirm that downstream targets of TCR, including VAV1, can lead to classically defined TCR downstream pathway target activation and subsequently induce apoptosis.

Discussion

PRL3 has been credentialed as a potent oncogene capable of driving elevated growth and metastasis in a wide range of cancer types. In gastric carcinoma, high PRL3 expression is associated with peritoneal and lymph node metastasis [15], while PRL3-positive breast carcinomas are associated with shorter disease-free survival and metastases [17]. In AML, PRL3 collaborates with activated FLT3 to elevate MAPK/ERK and STAT signaling, and is also associated with poor survival [40]. Here, we have uncovered that PRL3 is highly expressed in a subset of human T-ALLs and exhibits important roles in suppressing apoptosis through inhibiting phosphorylation of well-known downstream TCR signaling pathways. Furthermore, our work shows that PRL3 synergizes with the MYC oncoprotein to modify leukemia initiation, growth, and maintenance. Given the profound importance of PRL3 in cancer, it is surprising that PRL3-deficient mice are viable into adulthood and have largely normal blood cell function [41]. Collectively, this body of work suggests that direct targeting of PRL3 could be an effective therapeutic option for T- ALL and would be associated with a large and safe therapeutic window.

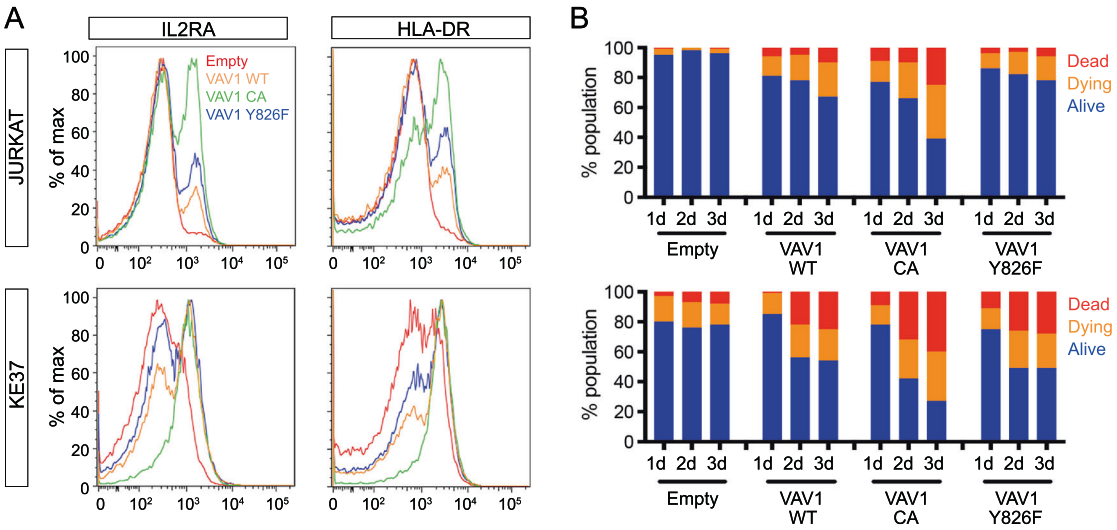

Fig. 7 Constitutively active VAV1 induces T-cell signaling pathways and subsequently induces apoptosis in both Jurkat and KE37 T-ALL cells. a Flow cytometry analysis showing T-cell activation marker IL2RA and HLA-DR expression after 2 days of nucleofection with empty control vector (Empty), wild-type VAV1 (VAV1 WT), constitutively active VAV1 (VAV1 CA), or unphosphorylatable VAV1 Y826F. **b** Quantification of Annexin-V/7AAD staining following 1, 2, or 3 days after nucleofection. Representative examples of three independent replicates are shown.

MYC is amplified in subset of human T-ALL and resides only 13.7 megabases from the PRL3 locus on chromosome 8q, raising the intriguing hypothesis that these two oncogenes might synergize to drive leukemia initiation and growth. Utilizing the zebrafish ALL model, we show that prl3 collaborated with Myc to initiate early-onset leukemia and enhance its aggression. Our results are in stark contrast to those reported by Wei et al. that report that PRL3 has no oncogenic role in the genesis of T-ALL, which might be ascribed to differences in strains of zebrafish used in each study or difficulty in ascribing lineage based on qRT-PCR [25, 28]. Our data also suggests that prl3 likely permits Myc-expressing lymphocytes to survive and ultimately to undergo transformation, likely through suppressing apoptosis. Indeed, analysis of prl3-transgenic T-ALLs revealed that leukemias had lower rates of apoptosis when compared with those that express only Myc. Finally, our work also showed that PRL3 is expressed at high levels in a substantial fraction of human T-ALL that do not contain 8q amplification and was required for their continued growth in vitro and in vivo, suggesting as of yet unidentified mechanisms by which PRL3 becomes expressed in human T-ALL. Taken together, our data strongly supports an oncogenic role for PRL3 in T-ALL and a requirement in the growth of a subset of human T-ALL. Our findings are in opposition with those recently reported by Wei et al. that suggested that PRL3 has no role in regulating T-ALL maintenance and growth, but rather regulates migration of human T-ALL [42]. This discrepancy is likely accounted for by differences in duration of follow up of knockdown cells in vitro, especially in light of results reported here and those presented by Wei et al. that PRL3 loss-of-function reduced xenograft growth in vivo [42]. Intriguingly, the MYC locus is also amplified in more than 25% of cases of breast cancer, colorectal cancer, esophageal cancer, head and neck cancer, hepatic cancer, and pancreatic cancer [43] and many of these tumors co-amplify PRL3, raising the interesting possibility that MYC and PRL3 may collaborate to drive malignant transformation in a variety of cancer types.

The process of TCR signaling is exquisitely controlled during T-cell maturation by both positive selection that results from retention of MHC reactive thymocytes through the activation of pro-survival signals and negative selection through the elimination of hyper-stimulated, autoreactive thymocytes. Elegant work from Trinquand et al. has shown that hyper-stimulation of TCR signaling can cause death of T-ALL cells in a manner consistent with elimination of autoreactive T cells during negative selection. These data suggest that TCR-signaling reactivation may be a potential therapeutic pathway in T-ALL [12] and provides a link to the mechanistic studies from our work showing that PRL3 can regulate classically defined downstream phosphorylation substrates of TCR signaling. During normal T-cell activation, TCR stimulation activates LCK, which leads to induction of a complex phosphorylation cascade that culminates in protein associations with the TCR that alter calcium mobilization, cytoskeleton rearrangement, Ras GTPase activation, transcription factor activation, and secretion of cytokines [44]. Our time-course experiments using a PRL3 inhibitor showed that several key T-cell signaling proteins were re-phosphorylated and subsequently

activated upon PRL3 inhibition, including VAV1, LAT, CBL, PLCγ1, and CD3D. These data support a model by which PRL3 inhibits the formation of the multi-protein signaling complex commonly associated with TCR activation. Remarkably Molt4 and KE37 cells lack intact, membrane active TCR and yet respond similarly to PRL3 knockdown as Jurkat cells that have an intact TCR. Collectively, our data suggest that PRL3 inhibits the self-assembly of the downstream signaling complexes and suppresses classical downstream TCR phosphorylation signaling in human T-ALL even in the absence of intact TCR. These data are similar in some regards to how calcium ionophore and phorbol esters activate downstream TCR phosphorylation signaling even in the absence of intact TCR [45, 46]. These findings are particularly exciting because we have now identified new signaling pathways classically defined as downstream effectors of TCR signaling as viable therapeutic targets in a large fraction of T-ALL and importantly, would not require leukemias to have an intact and functional TCR to elicit potent effects on cell death.

VAV1 is essential to TCR signaling and requires its GEF activity [31–33]. Aberrant activation of VAV1 through recurrent point mutations and gene fusions has suggested proto-oncogenic roles for VAV1 in peripheral T-cell lymphoma [47]. By contrast, VAV1 has tumor-suppressor roles in T-ALL where inactivation leads to elevated intracellular NOTCH1 signaling and transformation in the TLX+ subtype of T-ALL [48]. In keeping with the proposed tumor suppressive role for VAV1 in T-ALL, expression of constitutively active VAV1 led to elevated downstream TCR signaling and apoptosis, while GEF-inactive VAV1 Y826F did not elicit these responses. Intriguingly, our mass-spec phoshoproteomics data identified this same VAV1 Y826 residue as being rapidly phosphorylated after only 5 min of small molecule PRL3 inhibitor exposure, suggesting that VAV1 GEF activity may be directly suppressed by PRL3 phosphatase activity. Moreover, our gain-of-function experiments clearly show that the VAV1 can induce the downstream TCR-signaling phosphorylation substrates that are commonly repressed by PRL3 in human T-ALL to induce potent leukemia cell killing. In total, our work has identified novel and important roles for PRL3 in regulating T-ALL growth and maintenance, which is in part due to suppressing TCR phosphorylation substrates. Importantly, our results suggest that targeting the TCR/PRL3/VAV1 axis therapeutically would be a viable strategy in a large fraction of T-ALL.

Acknowledgements We thank Christina Luo, Hiranmayi Ravichandran, Rachel Servis, and Ravi Mylvaganam for technical assistance. We thank Drs. Finola Moore and Riadh Lobbardi for helpful discussion and thoughtful review of this manuscript. This work is supported by NIH grant R01CA211734 (DML), R37CA227656 (JSB), CA193651 (AG), the MGH Research Scholar Award (DML), Alex Lemonade Stand Foundation (JSB), the V Foundation for Cancer Research (AG), an Investigatorship from Boston Children's Hospital (AG), the Research Foundation Flanders (PVV, TT, SL), 'Kom op tegen Kanker' (Stand up to Cancer; SL), and the Ghent University Special Research Fund (PVV and TT). Flow cytometry services were supported by MGH Pathology CNY Flow Cytometry Core shared instrumentation grant 1S10RR023440-01A1.

Compliance with ethical standards

Conflict of interest The authors declare that they have no conflict of interest.

Publisher's note Springer Nature remains neutral with regard to jurisdictional claims in published maps and institutional affiliations.

References

1. Pui CH, Campana D, Pei D, Bowman WP, Sandlund JT, Kaste SC, et al. Treating childhood acute lymphoblastic leukemia without cranial irradiation. N Engl J Med. 2009;360:2730–41.
2. Pui CH, Evans WE. Treatment of acute lymphoblastic leukemia. N Engl J Med. 2006;354:166–78.
3. Belver L, Ferrando A. The genetics and mechanisms of T cell acute lymphoblastic leukaemia. Nat Rev Cancer. 2016;16:494–507.
4. Gianni F, Belver L, Ferrando A. The genetics and mechanisms of T-cell acute lymphoblastic leukemia. Cold Spring Harb Perspect Med. 2020;10:a035246.
5. Weng AP, Millholland JM, Yashiro-Ohtani Y, Arcangeli ML, Lau A, Wai C, et al. c-Myc is an important direct target of Notch1 in T-cell acute lymphoblastic leukemia/lymphoma. Genes Dev. 2006;20:2096–109.
6. Herranz D, Ambesi-Impiombato A, Palomero T, Schnell SA, Belver L, Wendorff AA, et al. A NOTCH1-driven MYC enhancer promotes T cell development, transformation and acute lymphoblastic leukemia. Nat Med. 2014;20:1130–7.
7. Ortega M, Bhatnagar H, Lin AP, Wang L, Aster JC, Sill H, et al. A microRNA-mediated regulatory loop modulates NOTCH and MYC oncogenic signals in B- and T-cell malignancies. Leukemia. 2015;29:968–76.
8. Marks DI, Paietta EM, Moorman AV, Richards SM, Buck G, Dewald G, et al. T-cell acute lymphoblastic leukemia in adults: clinical features, immunophenotype, cytogenetics, and outcome from the large randomized prospective trial (UKALLXII/ECOG 2993). Blood. 2009;114:5136–45.
9. Petit A, Trinquand A, Chevret S, Ballerini P, Cayuela JM, Grardel N, et al. Oncogenetic mutations combined with MRD improve outcome prediction in pediatric T-cell acute lymphoblastic leukemia. Blood. 2018;131:289–300.
10. Ko RH, Ji L, Barnette P, Bostrom B, Hutchinson R, Raetz E, et al. Outcome of patients treated for relapsed or refractory acute lymphoblastic leukemia: a therapeutic advances in childhood leukemia consortium study. J Clin Oncol. 2010;28:648–54.
11. Schrappe M, Hunger SP, Pui CH, Saha V, Gaynon PS, Baruchel A, et al. Outcomes after induction failure in childhood acute lymphoblastic leukemia. N Engl J Med. 2012;366:1371–81.
12. Trinquand A, Dos Santos NR, Quang CT, Rocchetti F, Zaniboni B, Belhocine M, et al. Triggering the TCR developmental checkpoint activates a therapeutically targetable tumor suppressive pathway in T-cell leukemia. Cancer Discov. 2016;6:973–85.
13. Bollu LR, Mazumdar A, Savage MI, Brown PH. Molecular pathways: targeting protein tyrosine phosphatases in cancer. Clin Cancer Res. 2017;23:2136–42.

14. Saha S, Bardelli A, Buckhaults P, Velculescu VE, Rago C, St. Croix B, et al. A phosphatase associated with metastasis of colorectal cancer. Science. 2001;294:1343–6.
15. Li ZR, Wang Z, Zhu BH, He YL, Peng JS, Cai SR, et al. Association of tyrosine PRL-3 phosphatase protein expression with peritoneal metastasis of gastric carcinoma and prognosis. Surg Today. 2007;37:646–51.
16. Zhao WB, Li Y, Liu X, Zhang LY, Wang X. Evaluation of PRL-3 expression, and its correlation with angiogenesis and invasion in hepatocellular carcinoma. Int J Mol Med. 2008;22:187–92.
17. Radke I, Götte M, Kersting C, Mattsson B, Kiesel L, Wülfing P. Expression and prognostic impact of the protein tyrosine phosphatases PRL-1, PRL-2, and PRL-3 in breast cancer. Br J Cancer. 2006;95:347–54.
18. Fiordalisi JJ, Keller PJ, Cox AD. PRL tyrosine phosphatases regulate Rho family GTPases to promote invasion and motility. Cancer Res. 2006;66:3153–61.
19. Liang F, Liang J, Wang WQ, Sun JP, Udho E, Zhang ZY. PRL3 promotes cell invasion and proliferation by down-regulation of Csk leading to Src activation. J Biol Chem. 2007;282:5413–9.
20. Kozlov G, Cheng J, Ziomek E, Banville D, Gehring K, Ekiel I. Structural insights into molecular function of the metastasis-associated phosphatase PRL-3. J Biol Chem. 2004;279:11882–9.
21. Rios P, Li X, Köhn M. Molecular mechanisms of the PRL phosphatases. FEBS J. 2013;280:505–24.
22. Ariës IM, Bodaar K, Karim SA, Chonghaile TN, Hinze L, Burns MA, et al. PRC2 loss induces chemoresistance by repressing apoptosis in T cell acute lymphoblastic leukemia. J Exp Med. 2018;215:3094–114.
23. Burns MA, Liao ZW, Yamagata N, Pouliot GP, Stevenson KE, Neuberg DS, et al. Hedgehog pathway mutations drive oncogenic transformation in high-risk T-cell acute lymphoblastic leukemia. Leukemia. 2018;32:2126–37.
24. Blackburn JS, Liu S, Raiser DM, Martinez SA, Feng H, Meeker ND, et al. Notch signaling expands a pre-malignant pool of T-cell acute lymphoblastic leukemia clones without affecting leukemia-propagating cell frequency. Leukemia. 2012;26:2069–78.
25. Garcia EG, Iyer S, Garcia SP, Loontiens S, Sadreyev RI, Speleman F, et al. Cell of origin dictates aggression and stem cell number in acute lymphoblastic leukemia. Leukemia. 2018;32:1860–5.
26. Wilsbacher JL, Moores SL, Brugge JS. An active form of Vav1 induces migration of mammary epithelial cells by stimulating secretion of an epidermal growth factor receptor ligand. Cell Commun Signal. 2006;4:1–13.
27. Borga C, Park G, Foster C, Burroughs-Garcia J, Marchesin M, Shah R, et al. Simultaneous B and T cell acute lymphoblastic leukemias in zebrafish driven by transgenic MYC: implications for oncogenesis and lymphopoiesis. Leukemia. 2019;33:333–47.
28. Borga C, Foster CA, Iyer S, Garcia SP, Langenau DM, Frazer JK. Molecularly distinct models of zebrafish Myc-induced B cell leukemia. Leukemia 2018;33:559–62.
29. Hara J, Benedict SH, Champagne E, Mak TW, Minden M, Gelfand EW. Comparison of T cell receptor α, β, and γ gene rearrangement and expression in T cell acute lymphoblastic leukemia. J Clin Investig. 1988;81:989–96.
30. Bajnok A, Ivanova M, Rigó J, Toldi G. The distribution of activation markers and selectins on peripheral T lymphocytes in preeclampsia. Mediators Inflamm. 2017;8045161.
31. Haubert D, Li J, Saveliev A, Calzascia T, Sutter E, Metzler B, et al. Vav1 GEF activity is required for T cell mediated allograft rejection. Transpl Immunol. 2012;26:212–9.
32. Wu J, Katzav S, Weiss A. A functional T-cell receptor signaling pathway is required for p95vav activity. Mol Cell Biol. 1995;15:4337–46.
33. Gulbins E, Coggeshall KM, Baier G. Tyrosine kinase-stimulated guanine nucleotide exchange activity of Vav in T cell activation. Science. 1993;260:822–5.
34. Lazer G, Pe'er L, Farago M, Machida K, Mayer BJ, Katzav S. Tyrosine residues at the carboxyl terminus of Vav1 play an important role in regulation of its biological activity. J Biol Chem. 2010;285:23075–85.
35. Wardenburg JB, Fu C, Jackman JK, Flotow H, Wilkinson SE, Williams DH, et al. Phosphorylation of SLP-76 by the ZAP-70 protein-tyrosine kinase is required for T-cell receptor function. J Biol Chem. 1996;271:19641–4.
36. Bustelo XR. Vav proteins, adaptors and cell signaling. Oncogene. 2001;20:6372–81.
37. Gulbins E, Coggeshall KM, Baier G, Telford D, Langlet C, Baier-Bitterlich G, et al. Direct stimulation of Vav guanine nucleotide exchange activity for Ras by phorbol esters and diglycerides. Mol Cell Biol. 1994;14:4749–58.
38. Helou YA, Petrashen AP, Salomon AR. Vav1 regulates T cell activation through a feedback mechanism and crosstalk between the T cell receptor and CD28. J Proteome Res. 2015;176:2963–75.
39. Aghazadeh B, Lowry WE, Huang XY, Rosen MK. Structural basis for relief of autoinhibition of the Dbl homology domain of proto-oncogene Vav by tyrosine phosphorylation. Cell. 2000;102:625–33.
40. Kobayashi M, Chen S, Gao R, Bai Y, Zhang ZY, Liu Y. Phosphatase of regenerating liver in hematopoietic stem cells and hematological malignancies. Cell Cycle. 2014;13:2827–35.
41. Zimmerman MW, Homanics GE, Lazo JS. Targeted Deletion of the metastasis-associated phosphatase Ptp4a3 (PRL-3) suppresses murine colon cancer. PLoS ONE. 2013;8:e58300.
42. Wei M, Haney MG, Rivas DR, Blackburn JS. Protein tyrosine phosphatase 4A3 (PTP4A3/PRL-3) drives migration and progression of T-cell acute lymphoblastic leukemia in vitro and in vivo. Oncogenesis. 2020;9:6.
43. Nicholson JM, Cimini D. Cancer karyotypes: survival of the fittest. Front Oncol. 2013;3:148.
44. Peterson EJ, Maltzman JS, Koretzky GA. T-cell activation and tolerance. In: Robert R. Rich editor. Clinical Immunology: Principles and Practice, 4th ed. USA: Elsevier Inc; 2013;160–71.
45. Nagasawa K, Howatson A, Mak TW. Induction of human malignant T-lymphoblastic cell lines MOLT-3 and jurkat by 12-O-tetradecanoylphorbol-13-acetate: biochemical, physical, and morphological characterization. J Cell Physiol. 1981;109:181–92.
46. Wang B, Kishihara K, Zhang D, Sakamoto T, Nomoto K. Transcriptional regulation of a receptor protein tyrosine phosphatase gene hPTP-J by PKC-mediated signaling pathways in Jurkat and Molt-4 T lymphoma cells. Biochim Biophys Acta—Mol Cell Res. 1999;1450:331–40.
47. Abate F, Da Silva-Almeida AC, Zairis S, Robles-Valero J, Couronne L, Khiabanian H, et al. Activating mutations and translocations in the guanine exchange factor VAV1 in peripheral T-cell lymphomas. Proc Natl Acad Sci USA. 2017;114:764–9.
48. Robles-Valero J, Lorenzo-Martín LF, Menacho-Márquez M, Fernández-Pisonero I, Abad A, Camós M, et al. A paradoxical tumor-suppressor role for the Rac1 exchange factor Vav1 in T cell acute lymphoblastic leukemia. Cancer Cell. 2017;32:608–23.